Thermoelectric properties of partly Sb- and Zn-substituted Ba$_8$Ga$_{16}$Ge$_{30}$ clathrates

D. Cederkrantz,[1,a)] M. Nygren,[2] and A. E. C. Palmqvist[1]

[1]*Department of Chemical and Biological Engineering, Chalmers University of Technology, SE-41296 Göteborg, Sweden*
[2]*Department of Inorganic Chemistry, Arrhenius Laboratory, Stockholm University, SE-10691 Stockholm, Sweden*

The effects on the thermoelectric properties of n-Ba$_8$Ga$_{16}$Ge$_{30}$ when substituting small amounts of the Ga or Ge with Sb or Zn have been investigated. A number of syntheses were prepared in quaternary systems of Ba$_8$Ga$_{16}$Ge$_{30}$ substituted with either Sb or Zn but only three samples were found to yield single phase products with nominal compositions of Ba$_8$Ga$_{15}$Sb$_1$Ge$_{30}$, Ba$_8$Ga$_{15}$Zn$_1$Ge$_{30}$ and Ba$_8$Ga$_{16}$Ge$_{28}$Zn$_2$, respectively. When Ge was substituted for Zn the resulting sample remained n-type and an increase in thermopower and a decrease in thermal conductivity were achieved. These positive effects were accompanied with an increased electrical resistivity and thus the ZT was only somewhat improved up to about 400 °C. When substituting Ga with either Sb or Zn samples remained n-type but showed decreased thermopower and increased electrical resistivity and thermal conductivity. It is thus concluded that substitution of Ga with Zn or Sb is detrimental for the thermoelectric properties of Ba$_8$Ga$_{16}$Ge$_{30}$, whereas substitution of Ge with Zn appears a potent method for improving its performance. © *2010 American Institute of Physics*. [doi:10.1063/1.3518043]

I. INTRODUCTION

The worldwide demand for energy is expected to continue to increase in the foreseeable future and as fossil fuel resources approach peak production rates the energy price will likely increase. The increasing energy cost opens the market to more exotic energy conversion technologies and among them thermoelectric generators (TEGs). These utilize materials that can convert a difference in temperature directly into an electrical potential that can drive an electrical current. Consequently, a possible and desirable application of TEGs is waste heat recovery, where they benefit from compact design, with no moving parts, and a long life time.[1] On the downside are potentially expensive thermoelectric materials and relatively poor conversion efficiencies (<10% in most cases).[2] These characteristics make thermoelectric heat recovery suitable for use in automotive applications, where improved fuel economy is very important along with compact size and low operational weight.

The performance of a thermoelectric material is characterized by its Seebeck coefficient (S), electrical conductivity (σ) and thermal conductivity (κ). These can be combined in the dimensionless figure-of-merit $ZT=TS^2\sigma/\kappa$, where T is the absolute temperature of operation.[3,4] The materials commercially used today were mainly developed during the space race in the 1960s. In the mid 1990s, thermoelectric materials research received a boost in interest when the "phonon-glass electron-crystal" concept was presented by Slack.[5] This suggests that a good thermoelectric material should conduct heat like a glass and electricity like a crystal and that host-guest crystal structures with loosely bound

"rattling" atoms should show such properties. One group of thermoelectric materials that has attracted much interest in this context is the semiconducting clathrates, which are host-guest structures, where the guest atoms are positioned in somewhat oversized cages or cavities formed by the host lattice.[6,7] The research spent on this group of materials has been quite extensive and considerable progress has been made, where an n-doped type-I clathrate Ba$_8$Ga$_{16}$Ge$_{30}$ with a ZT of 1.35 at 900 K is one of the most promising results.[8]

While n-type clathrates have been developed successfully there is a lack of p-type clathrates. This is because the structure disfavors bonds between trivalent atoms (Ga in the case of Ba$_8$Ga$_{16}$Ge$_{30}$), which pushes the favored element composition ratio of the host structure toward the tetravalent atom (Ge in Ba$_8$Ga$_{16}$Ge$_{30}$). This results in excess electrons in the structure and thus n-type behavior.[9] Despite this p-type clathrates can be synthesized, but as we have reported earlier they suffer from stability problems at high temperatures.[10] Finding more stable p-type materials or further improving the properties of the thermoelectric clathrates usually involves partial or complete substitution of one of the host atoms and forming new ternary[11–15] or quaternary[16–20] systems. Introduction of a fourth element to the system could affect band structure and through this the electrical and thermal properties. Such elements can be Zn, which is a lighter element with fewer valence electrons than both host atoms, Ga and Ge, in Ba$_8$Ga$_{16}$Ge$_{30}$ or Sb which is heavier and has more valence electrons compared to both Ga and Ge. In this paper, we study the impact on the thermoelectric properties of Ba$_8$Ga$_{16}$Ge$_{30}$ when substituting Ga or Ge with Zn and Sb in a direct solid state reaction synthesis.

a)Electronic mail: daniel.cederkrantz@chalmers.se.

TABLE I. Nominal elemental compositions of synthesized samples.

Sample ID	Nominal composition
G1	$Ba_8Ga_{16}Ge_{30}$
S1	$Ba_8Ga_{15}Sb_1Ge_{30}$
Z1	$Ba_8Ga_{15}Zn_1Ge_{30}$
Z2	$Ba_8Ga_{16}Ge_{28}Zn_2$

II. EXPERIMENTAL

A. Synthesis

The synthesis of clathrate samples was done by direct reactions of high-purity elements, Ba (99.99%), Ga (99.9995%), Ge (99.9999%), Sb (99.999%), and Zn (99.9999%) all from Sigma-Aldrich. A large number of syntheses were prepared but only the ones resulting in single phase products are described in Table I. For these, stoichiometric amounts in accordance with the compositions found in Table I were used except for sample G1 where a 2.5 wt % Ba excess was added to avoid the formation of the characteristic Ge impurity phase and thus achieve a single phase system.[21] Mixing of the elements was performed in a glove box (high purity Ar atmosphere). All samples were prepared in alumina crucibles and this reaction vessel was subsequently placed in a sealed quartz tube, under argon atmosphere. The tube was then evacuated to a pressure of approximately 0.1 mbar and placed in a furnace (Thermolyne 21 100 tube furnace equipped with a Eurotherm controller) and heated to 1050 °C over 10 h and kept there for 1 h, cooled to 970 °C over 1.5 h followed by a slow approach over 4 h to the annealing temperature (963 °C). The annealing time was 24 h and followed by a slow cooling over 3 h to 955 °C and subsequently a more rapid cooling to room temperature. After completed synthesis the formed crystals were crushed to enable their removal from the crucible.

B. Powder x-ray diffraction (XRD)

Powder XRD was performed on ground samples using a Bruker XRD D8 Advance and monochromatic Cu $K_{\alpha 1}$ radiation. Data were collected on powders before sintering and on the disks after sintering covering the 2θ range 17°–60° and for selected samples 10°–120°.

C. Sample preparation

To enable property measurements selected samples, G1, S1, Z1, and Z2 were ground (by mortar and a Mixer Mill MM400 from Retch), sintered with SPS (Dr Sinter 2050, SPS Syntex Inc., Japan) and cut into suitable specimens for analysis. The polycrystalline samples were sintered in graphite dies at 750 °C (S1) or 800 °C (G1, Z1, and Z2) for 5 min using a pressure of 100 MPa, which resulted in disks with a diameter of 12 mm, a thickness in the range of 2.3–2.6 mm and a density >95% of the theoretical. For measurement of the thermal conductivity, the disks were used directly after polishing, while for the electrical property measurements they were cut into rods with sides of 2–4 mm and a length of 9–11 mm using a diamond saw.

D. Thermal conductivity measurement

The thermal conductivity measurements were executed with a Hot Disk TPS 2500 S unit using the transient plane source (TPS) method.[22] For this method, a thin disk-shaped sensor, or element, is used. The element has a known temperature-dependent resistivity and serves as both heating element for the measurements and temperature sensor. The technique is based on three-dimensional heat flow inside a sample, which, by limiting the total time of transient recording, can be regarded as an infinite medium. Normally, the TPS-sensor is sandwiched between two identical samples to have uniform heat dissipation from both sides of the sensor during the measurements, but due to limited sample amounts single sided measurements had to be performed for most samples in this study. This means that a TPS-element was sandwiched between the sample and a support material which has a very low thermal conductivity; in this case styrofoam was used at room temperature and porous furnace insulation was used for measurements at elevated temperatures. Using this technique, essentially all heat produced by the TPS-sensor will dissipate into the sample since it has the greater thermal conductivity, thus giving an accurate measurement of its thermal conductivity. Measurements were performed initially in open atmosphere at room temperature and following that under helium atmosphere at temperatures up to 650 °C. At each temperature the measurement was repeated three times and the calculated average is the presented value. For the room temperature measurements, a 3.189 mm diameter Ni TPS-element with Kapton insulation was used, while a Ni element of 3.189 mm diameter insulated with mica was used for measurements at elevated temperatures. The results from measurements with the mica sensor were calibrated with the room temperature measurements performed with the Kapton sensor and compared to available double sided measurements to achieve a stable baseline for the measurements performed at elevated temperatures. Room temperature data from the different sensor types were compared and a correction factor was calculated for each sample and then used to adjust the high temperature measurements accordingly.

E. Electrical properties

The Seebeck coefficient (S) and the electrical resistivity $(1/\sigma)$ were measured simultaneously with a ZEM-3 instrument manufactured by Ulvac-Riko, Inc. All measurements were performed in low pressure He atmosphere in a temperature range from room temperature to 650 °C. To measure the thermopower a static dc method is used by obtaining a potential difference (ΔV) induced by a temperature difference (ΔT) over a well defined length of the sample rod, which gives $S=\Delta V/\Delta T$. Resistivity is calculated from the resistance obtained by the 4-point probe method (R=V/I), the known cross section area (A) and the distance between the voltage probes (d) using the relation $1/\sigma=R\times A/d$.

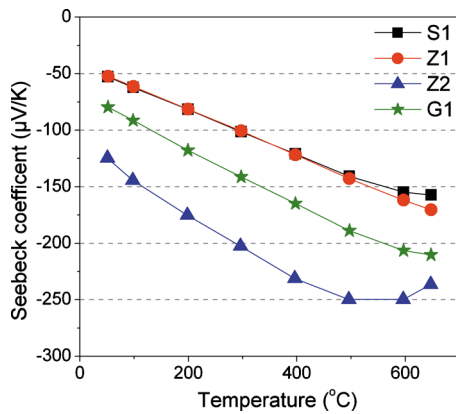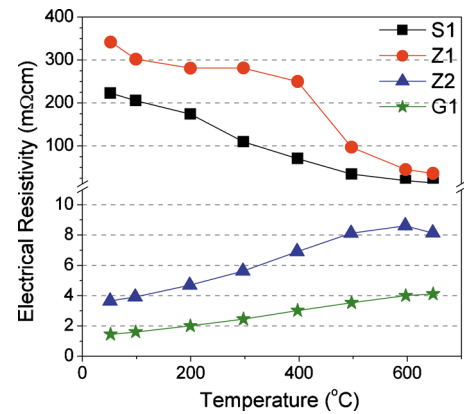FIG. 1. (Color online) Seebeck coefficient of samples described in Table I.

FIG. 2. (Color online) Electrical resistivity of the samples presented in Table I. Z2 and G1 have typical heavily doped semiconductor behavior, while S1 and Z1 are very poor semiconductors with high electrical resistivity.

III. RESULTS AND DISCUSSION

A. Sample preparation and characterization

The XRD patterns of the samples agreed well with the previously reported $Ba_8Ga_{16}Ge_{30}$ structure,[21,23,24] but for several syntheses substantial amounts of impurity phases of mainly GaSb and a diffuse Zn phase were present. For this reason only samples S1, Z1, and Z2, which showed no presence of any impurity phase in their XRD diffractograms, were analyzed further together with the unsubstituted sample G1 for thermoelectric evaluation. The presence of these impurity phases and possible evaporation during synthesis make exact elemental composition of the sample somewhat uncertain, but for simplicity references will be done to the nominal composition used in the syntheses. The disks prepared by SPS were dense and homogenous, and the cutting of the samples did not reveal any cracks. The Scherrer formula[25] was used to get a rough estimate of the minimum grain size in the sintered samples from the XRD measurements. The analysis of the sintered samples showed no significant peak broadening compared to the ground powder, which has a particle size of several micrometers, and the grains in the sintered disks were therefore concluded to be of similar size.

B. Thermoelectric evaluation

1. Thermopower

In Fig. 1, the Seebeck coefficient of the measured samples is presented as a function of temperature. It is clear that all samples were n-doped, and that Z2 showed the highest absolute Seebeck value, while for samples S1 and Z1 the thermopower was very similar and comparably low. The latter two samples are both substituting Ga and it would seem that the addition of small amounts of either Zn or Sb have a surprisingly similar effect on the Seebeck coefficient. The n-doping is expected for the Sb substitution since it will contribute with more electrons to the structure compared to Ga. For Zn substitution, on the other hand, p-doping could be expected if the Zn can replace Ga in the structure and act as an electron acceptor. But if the nominal composition is not reached or Zn does not enter the structure the Ga/Ge ratio will be less than 16/30 that in turn results in n-doping,[9,26] a scenario that is not unlikely. When the substitution was in-

stead performed for Ge a significant improvement of the Seebeck coefficient occurred. For sample Z2 a value of -250 $\mu V/K$ was reached between 500 and 600 °C and the peak temperature was reached earlier than for the other systems which all appeared to peak somewhere outside the measured range, i.e., above 650 °C. It has previously been reported that Zn substitution for Ge results in p-type behavior,[16] in contrast to what sample Z2 exhibits. The n-type behavior is intriguing since even if no Zn entered the structure the sample is expected to be p-type because the Ga/Ge ratio used is larger than 16/30. Judging from Fig. 1, it is, however, clear that the Zn has an effect on the sample apparently different from that in the sample reported previously, possibly as a result of differences in synthesis details employed. The lower peak temperature of Z2 compared to G1 indicates a reduced charge carrier concentration, which is in agreement with an increased electrical resistivity and a reduced thermal conductivity compared to the pure $Ba_8Ga_{16}Ge_{30}$ sample (G1) as shown later. The sample G1 has the expected behavior of an n-type $Ba_8Ga_{16}Ge_{30}$ sample and compares very well with previously published thermopower data.[10,27,28]

2. Electrical resistivity

The electrical resistivity was found to differ greatly between the samples as seen in Fig. 2. Samples Z2 and G1 both have rather low electrical resistivity with a typical behavior of heavily doped semiconductors with resistivity increasing toward a maximum where the intrinsic transition sets.[29] The somewhat higher resistivity and the lower peak temperature of Z2 further support a slightly lower charge carrier concentration compared to the unsubstituted G1 sample. For the other two samples, S1 and Z1, a surprisingly high electrical resistivity is measured with room temperature resistivity roughly a factor 100 higher than for samples Z2 and G1. The analysis of the XRD data shows similar size of the grains in the range of several micrometers for all samples. Since the expected mean free path of charge carriers in $Ba_8Ga_{16}Ge_{30}$ and other similar clathrates is in the range of 1–300 Å at 2 K and is reduced with temperature[30–32] it is concluded that grain size effects cannot explain the behavior of the resistiv-
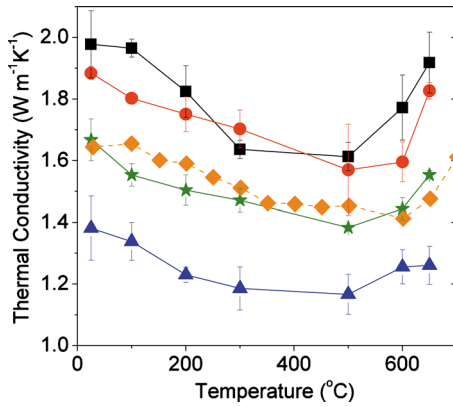
FIG. 3. (Color online) Total thermal conductivity of samples S1 (■), Z1 (●), Z2 (▲), and G1 (★) presented in Table I compared with a previously published (Ref. 10) n-doped $Ba_8Ga_{16}Ge_{30}$ sample, n-ref (◆). The standard deviation for all TPS data points is less than 10%.

FIG. 4. (Color online) Thermal conductivity divided into κ_l (—) and κ_{cc} (- -) using the Wiedemann–Franz relation for samples S1 (■), Z1 (●), Z2 (▲), and G1 (★) presented in Table I.

ity or any of the other properties. The high resistivity rather indicates a lower charge carrier concentration in these samples or possibly alteration of properties at interfaces or grain boundaries that limits the propagation of charge carriers in the sample. The reason for this increase in electrical resistivity must be related to the substitution, since it has previously been reported that reducing the amount of Ga in the structure should result in a more conducting material.[26] The exact reason for the increased electrical conductivity has not been determined but it is interesting to note that this increase is coupled with a decrease in the Seebeck coefficient. In a homogenous material, it is expected that the thermopower increases when moving toward a more electrically insulating material,[7] something clearly not seen here. We can therefore speculate that the substituent instead of taking the position of Ga rather segregates to grain boundaries and thus limits conduction through higher contact resistance between grains.

3. Thermal conductivity

The thermal conductivities for all measured samples are presented in Fig. 3 together with previously published thermal conductivity data of a comparable n-type $Ba_8Ga_{16}Ge_{30}$ sample[10] measured with a conventional Laser Flash instrument. The reference sample and sample G1 were synthesized following the same method, but are from different batches. It is therefore expected that they have similar thermal conductivity. All samples exhibit the expected semiconductor behavior with an initial drop in thermal conductivity, which reaches a minimum followed by a subsequent increase in conductivity. The increase in thermal conductivity is indicative of the intrinsic transition and the onset of conduction with both electrons and holes. When comparing the samples doped with Zn, Z1, and Z2, it is clear that the thermal conductivity is affected differently depending on which host atom Zn replaces. With substitution of Ge (Z2) a decrease in thermal conductivity by 17% was achieved at room temperature supporting the assumption that the charge carrier concentration is reduced compared to the G1 sample. When substitution is performed for Ga, on the other hand, an increase of 13% and 19% for Z1 and S1, respectively, was induced at
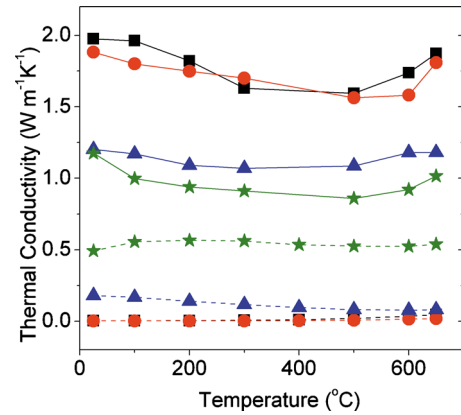
room temperature compared to the unsubstituted sample. It is interesting to note that the samples S1 and Z1 have the highest thermal conductivity, considering that they have the lowest electrical conductivity. The total thermal conductivity is the sum of the contribution from charge carriers (κ_{cc}) and lattice vibrations (κ_l), as seen in Eq. (1). κ_{cc} can be estimated with the Wiedemann–Franz law seen in Eq. (2), with the use of the Lorenz factor (L) and the electrical resistivity ($1/\sigma$). Subtracting κ_{cc} from the measured thermal conductivity κ_l can be obtained

$$\kappa = \kappa_{cc} + \kappa_l, \tag{1}$$

$$\kappa_{cc} = L\sigma T. \tag{2}$$

For calculating κ_{cc} a value of $L=2.4$ J^2 K^{-2} C^{-2} for free electrons was used[7] and the result is presented in Fig. 4. It is clear that S1 and Z1 both have a very low or insignificant contribution from the charge carriers to the thermal conductivity, of course as a result of the high electrical resistivity. As a result κ_l of S1 and Z1 is more or less double that of G1 and Z2. It can therefore be proposed that substituting Ga with either Sb or Zn improves the propagation of phonons in the structure, while this seems to occur to a much lower extent when substituting Ge. The reason for this remains to be investigated.

4. Figure of merit, ZT

The figure of merit, ZT, was calculated from the presented results and is shown in Fig. 5. Z2 and the unsubstituted sample G1 have fairly equal ZT values up to around 500 °C where the intrinsic transition sets in for Z2, which peaks at ZT=0.51 at 500 °C. It can be noted that Z2 has a slightly higher ZT value from room temperature to 300 °C, and thus compensates its higher resistivity with lower thermal conductivity and higher thermopower in this temperature range. Above 400 °C the decrease in thermopower of Z2 sets in and this combined with the sharper increase in electrical resistivity allow the ZT of the G1 sample to be higher, reaching a value of 0.64 at the peak temperature 600 °C. For the samples S1 and Z1, all three thermoelectric parameters work against a reasonable ZT value. Especially, the high
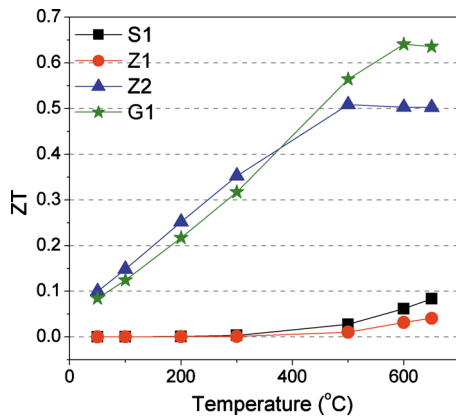
FIG. 5. (Color online) ZT values calculated from the presented results for the samples described in Table I.

electrical resistivity is a problem at temperatures below 500 °C, above which the ZT increased somewhat as the electrical resistivity decreases.

IV. CONCLUSIONS

Partly substituting Ga or Ge with Sb or Zn in $Ba_8Ga_{16}Ge_{30}$ through solid state reaction synthesis can result in single phase systems if the synthesis conditions are right. This study shows that Zn substitution on the Ge position results in enhanced thermopower and also lower thermal conductivity compared to the unsubstituted n-$Ba_8Ga_{16}Ge_{30}$. Counteracting these positive effects is an increased electrical resistivity and seemingly a lower charge carrier concentration shifting the ZT peak value to a lower temperature. As a result ZT is comparably high up to 400–500 °C and then levels off. It is expected that ZT may be improved further by optimization of the Zn content in the $Ba_8Ga_{16}Ge_{30-x}Zn_x$ system. When substituting on the Ga position on the other hand, an overall negative trend was observed for all the thermoelectric properties. It is puzzling that the thermopower is reduced at the same time as the electrical conductivity, a trend not normally expected. Since the electrical conductivity increased with a factor larger than 100 when substituting either Sb or Zn it is reasonable to argue that the charge carrier transport has been hampered since the intrinsic transition was not reached at lower temperatures than for the unsubstituted system as would have been expected for the alternative explanation of a decreased charge carrier concentration.

[1] D. M. Rowe, in *CRC Handbook of Thermoelectrics*, edited by D. M. Rowe (CRC, Boca Raton, 1995).
[2] L. E. Bell, Science **321**, 1457 (2008).
[3] A. F. Ioffe, *Semiconductor Thermoelements and Thermoelectric Cooling* (Infosearch Ltd., London, 1957).
[4] H. J. Goldsmid, in *CRC Handbook of Thermoelectrics*, edited by D. M. Rowe (CRC, Boca Raton, FL, 1995).
[5] G. A. Slack, in *CRC Handbook of Thermoelectrics*, edited by D. M. Rowe (CRC, Boca Raton, FL, 1995).
[6] H. Kleinke, Chem. Mater. **22**, 604 (2010).
[7] G. J. Snyder and E. S. Toberer, Nature Mater. **7**, 105 (2008).
[8] A. Saramat, G. Svensson, A. E. C. Palmqvist, C. Stiewe, E. Mueller, D. Platzek, S. G. K. Williams, D. M. Rowe, J. D. Bryan, and G. D. Stucky, J. Appl. Phys. **99**, 023708 (2006).
[9] M. Christensen and B. B. Iversen, Chem. Mater. **19**, 4896 (2007).
[10] D. Cederkrantz, A. Saramat, G. J. Snyder, and A. E. C. Palmqvist, J. Appl. Phys. **106**, 074509 (2009).
[11] A. Bentien, E. Nishibori, S. Paschen, and B. B. Iversen, Phys. Rev. B **71**, 144107 (2005).
[12] S. Johnsen, A. Bentien, G. K. H. Madsen, M. Nygren, and B. B. Iversen, *Proceedings of the 24th International Conference on Thermoelectrics* (IEEE, New York, 2005), pp. 211–214.
[13] N. Melnychenko-Koblyuk, A. Grytsiv, L. Fornasari, H. Kaldarar, H. Michor, F. Rohrbacher, M. Koza, E. Royanian, E. Bauer, P. Rogl, M. Rotter, H. Schmid, F. Marabelli, A. Devishvili, M. Doerr, and G. Giester, J. Phys.: Condens. Matter **19**, 216223 (2007).
[14] H. Anno, M. Hokazono, H. Takakura, and K. Matsubara, *Proceedings of the 24th International Conference on Thermoelectrics* (IEEE, New York, 2005), pp. 102–105.
[15] T. Uemura, K. Akai, K. Koga, T. Tanaka, H. Kurisu, S. Yamamoto, K. Kishimoto, T. Koyanagi, and M. Matsuura, J. Appl. Phys. **104**, 013702 (2008).
[16] S. K. Deng, X. F. Tang, and Q. J. Zhang, J. Appl. Phys. **102**, 043702 (2007).
[17] H. Anno, M. Hokazono, M. Kawamura, and K. Matsubara, *Proceedings of the 22nd Conference on Thermoelectrics* (IEEE, New York, 2003), pp. 121–126.
[18] S. K. Deng, X. F. Tang, P. Li, and Q. J. Zhang, J. Appl. Phys. **103**, 073503 (2008).
[19] K. Suekuni, S. Yamamoto, M. A. Avila, and T. Takabatake, *Proceedings of the 26th International Conference on Thermoelectrics* (IEEE, New York, 2007), pp. 234–236.
[20] D. Shukang, T. Xinfeng, L. Han, Y. Yonggao, and Z. QingJie, *Proceedings of the 26th International Conference on Thermoelectrics* (IEEE, New York, 2007), pp. 230–233.
[21] A. Saramat, E. S. Toberer, A. F. May, and G. J. Snyder, J. Electron. Mater. **38**, 1423 (2009).
[22] S. E. Gustafsson, Rev. Sci. Instrum. **62**, 797 (1991).
[23] B. Eisenmann, H. Schafer, and R. Zagler, J. Less-Common Met. **118**, 43 (1986).
[24] J. L. Cohn, G. S. Nolas, V. Fessatidis, T. H. Metcalf, and G. A. Slack, Phys. Rev. Lett. **82**, 779 (1999).
[25] A. L. Patterson, Phys. Rev. **56**, 978 (1939).
[26] H. Anno, M. Hokazono, M. Kawamura, J. Nagao, and K. Matsubara, *Proceedings of the 21st International Conference on Thermoelectrics* (IEEE, New York, 2002), pp. 77–80.
[27] N. L. Okamoto, K. Kishida, K. Tanaka, and H. Inui, J. Appl. Phys. **100**, 073504 (2006).
[28] M. Christensen, G. J. Snyder, and B. B. Iversen, *Proceedings of the 25th International Conference on Thermoelectrics* (IEEE, New York, 2006), pp. 40–43.
[29] E. S. Toberer, M. Christensen, B. B. Iversen, and G. J. Snyder, Phys. Rev. B **77**, 075203 (2008).
[30] A. Bentien, M. Christensen, J. D. Bryan, A. Sanchez, S. Paschen, F. Steglich, G. D. Stucky, and B. B. Iversen, Phys. Rev. B **69**, 045107 (2004).
[31] A. Bentien, V. Pacheco, S. Paschen, Y. Grin, and F. Steglich, Phys. Rev. B **71**, 165206 (2005).
[32] A. Bentien, S. Johnsen, and B. B. Iversen, Phys. Rev. B **73**, 094301 (2006).